Appl. Phys. A (2015) 118:1153–1160
DOI 10.1007/s00339-014-8931-0

Applied Physics A
Materials Science & Processing

Electrical resistivity change in amorphous $Ta_{42}Si_{13}N_{45}$ films by stress relaxation

M.-A. Nicolet · M. Ryser · V. Romano

Received: 18 June 2014 / Accepted: 11 December 2014 / Published online: 25 December 2014

Abstract In a first experiment, a reactively sputtered amorphous $Ta_{42}Si_{13}N_{45}$ film about 260 nm thick deposited on a flat and smooth alumina substrate was thermally annealed in air for 30 min and let cooled again repeatedly at successively higher temperatures from 200 to 500 °C. This treatment successively and irreversibly increases the room temperature resistivity of the film monotonically from its initial value of 670 μΩ cm to a maximum of 705 μΩ cm (+5.2 %). Subsequent heat treatments at temperatures below 500 °C and up to 6 h have no further effect on the room temperature resistivity. The new value remains unchanged after 3.8 years of storage at room temperature. In a second experiment, the evolution of the initially compressive stress of a film similarly deposited by reactive sputtering on a 2-inch silicon wafer was measured by tracking the wafer curvature during similar thermal annealing cycles. A similar pattern of irreversible and reversible changes of stress was observed as for the film resistivity. Transmission electron micrographs and secondary ion mass profiles of the film taken before and after thermal annealing in air establish that both the structure and the composition of the film scarcely change during the annealing cycles. We reason that the film stress is implicated in the resistivity change. In particular, to interpret the observations, a model is proposed where the interface between the film and the substrate is mechanically unyielding.

M.-A. Nicolet (✉)
California Institute of Technology, Pasadena, CA 91125, USA
e-mail: man@caltech.edu

M. Ryser · V. Romano
Institute of Applied Physics, University of Bern, 3012 Bern, Switzerland

V. Romano
Bern University of Applied Sciences, 3400 Burgdorf, Switzerland

1 Introduction

Films of atomic composition $Ta_{42}Si_{13}N_{45}$ reactively sputter deposited are structurally amorphous even under high-resolution transmission electron microscopy [1, 2]. A remarkable property of such films is that they withstand crystallization upon vacuum annealing for 30 min at temperatures as high as 800 °C [2, 3]. One would surmise that such a high structural metastability would warrant a good thermal stability of the electrical resistivity of the film as well. The present experimental study was performed to test that idea. As will be seen, this is not the case. However, if the film and substrate assembly are suitably pre-annealed, the TaSiN film becomes attractive as an electronic element exposed to harsh surroundings and/or to frequent temperature cycling.

2 Experimental procedures

The film was deposited by *rf* sputtering in an Ar/N_2 discharge from a 7.5 cm diameter Ta_5Si_3 target onto an electrically and thermally floating alumina substrate. Analysis by 1.4 MeV $^4He^{++}$ backscattering spectrometry of films deposited under the same conditions on carbon substrates established an atomic composition of Ta:Si:N = 42:13:45 with a few atm% of argon and little oxygen mixed in. The film is about 260 nm thick.

The substrate consisted of highly polished 1.0 mm thick alumina 5.1 by 5.1 cm^2 in size. After film deposition, well-spaced square samples of the film 9.20 × 9.20 mm^2 were

formed by photoresist patterning and chemical etching. Then, individual samples of 9.6 × 9.6 mm^2 each in size were cut out with a diamond saw. A probe with four linearly aligned points and 1-mm spacing was used together with absolutely calibrated volt and ampere meters to measure the resistance of the film at room temperature. Direct currents in the range of + and −1 to 9 mA yielded readily measurable voltages with insignificant heating of the film and a confirmed linearity of voltage versus current over that decade of values, and even much beyond. A linear regression taken over voltage values measured for each mA from −9 to +9 mA yielded the values quoted in Table 1.

Repeated readings with fixed probe position differed by about 0.2 %. When the linear four-point probe was repositioned parallel and halfway to either pair of edges of the square film, the measured values differed between 0.1 and 0.5 % at most. Data obtained with a diagonal centering of the probe also fell in that range. In all, the typical precision of the readings is within ±0.2 %.

Samples were thermally annealed in a tube furnace equipped with an open ceramic tube of 4.0 mm inner diameter and 42 cm length. The tube was heated over the center 38 cm. The temperature profile at the center of the tube where the sample was placed was uniform within 0.5 °C over the size of the sample. It rested in a small open glass boat with which it was inserted in the tube and removed from it while the temperature was held at a constant value of between about 200–500 °C. The actual temperature of annealing was determined with a chromel-constantan (type E, Ni90Cr10–Ni55Cu45) thermocouple made of fine 150 μm wires to minimize heat losses. The thermocouple joint and the sample rested in immediate proximity to each other in the glass boat. The readings were accurate within 1 or 2 °C as referenced to a couple in an ice/water bath.

3 Results

Table 1 gives the timeline of the experiment in row 1. The aim of this sequence of annealing steps is to subject a sample to sequentially higher temperatures, or repeated temperatures, up to 500 °C and then follow with annealing below 500 °C. The numbers in that row indicate on what day after the beginning of the experiment an annealing step was executed, always on the same sample. The annealing step (row 2), its duration in minutes, unless stated otherwise (row 3), and the annealing temperature (row 4) are specified. After each annealing step, the sample was left to cool to room temperature and stored at room temperature. At least 30 min elapsed after an annealing step before a next measurement was performed. Tests verified that beyond that cooling period, the readings were constant. Sometimes measurements were repeated just prior to the next annealing step to verify that long-term effects during storage at room temperature were absent. Row 5 reports the result of a measurement obtained after the corresponding annealing step. R is the result of a linear regression analysis of the ratios of the voltage measured between the inner pair and the currents passing through the outer pair of the four-point probe taken over the range of ±9 mA of probe currents. Step 12 was taken after a period of 15 days during which the sample had rested at room temperature. Step 16 gives data recorded at room temperature after the film had been stored at room temperature for 3.8 years past the last annealing of step 15. Annealing durations lasted 30 min for steps 1–8; subsequent annealing steps lasted (much) longer.

To visualize the results of Table 1, the annealing temperatures in row 4 are plotted for each step in Fig. 1a. Figure 1b gives values of R recorded after the indicated heat treatment. Multiplying R by $\pi/\ln 2$ yields the sheet resistance ρ_s in Ω/square of the film. This quantity is shown on the right ordinate of Fig. 1b. That multiplication assumes that the film extends much beyond the size of the four-point probe. This condition is not satisfied with the 9.20 mm^2 sample size and the 3 mm wide linear four-point probe.

Smits [4] has calculated the correction that should be applied when the extent of the film is commensurable with the width of the four-point probe. For the present case, the sheet resistivity reported in Fig. 1b should thus be reduced by about 7 % to get its actual value. This correction was

Table 1 Temporal sequence of measurements and results

Annealing	Day	1	5	7			8			9	12	13	+15	29	30		+3.8 years
Step	0	1	2	3	4	5	6	7	8	9	10	11	12	13	14	15	16
Duration (min)		30	30	30	30	30	30	30	30	150	360	330	15 days	120	150	60	3.8 years
Temperature (°C)	*rt*	190	300	298	394	396	392	490	490	350	348	395	*rt*	301	394	396	*rt*
R (Ω) = 6.00+	0.09	0.13	0.18	0.20	0.23	0.29	0.30	0.38	0.41	0.41	0.45	0.42	0.42	0.42	0.46	0.42	0.39

Data on the sequential annealing steps in air of the amorphous $Ta_{42}Si_{13}N_{45}$ film. *First row* day on which a particular annealing step took place after the start of the experiment. *Second row* numerical order of the sequential annealing steps. *Third row* duration of a particular annealing step in minutes, unless noted otherwise. *Fourth row* temperature of a particular annealing step. *Fifth row* value of R measured *after* a particular annealing step. R is the ratio of the DC voltage measured between the two inner probes and the DC current passing through the two outer probes of the linear four-point probe

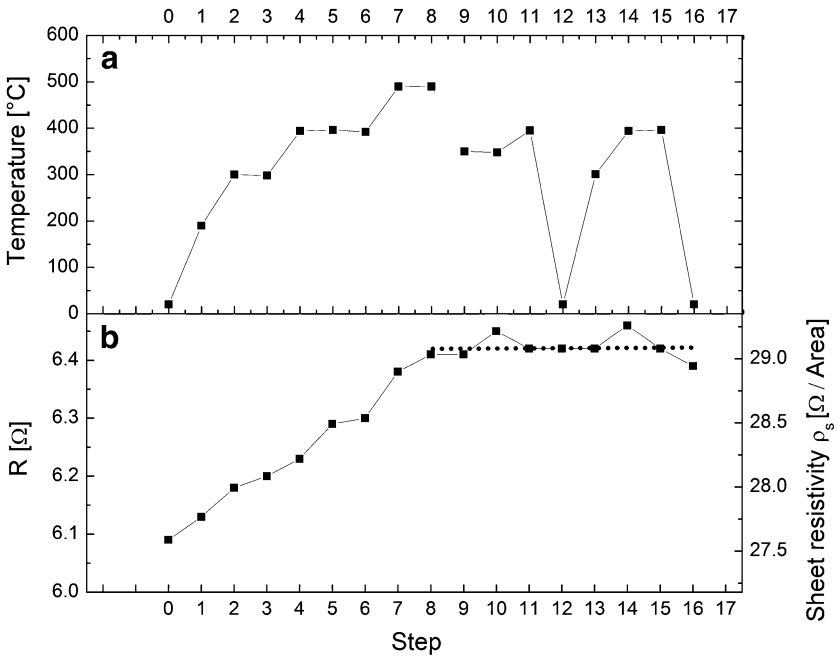

Fig. 1 Graphical rendition of the data in Table 1. **a** Annealing temperatures as a function of the annealing step as reported in Table 1. Annealing steps 1 to 8 all lasted 30 min. Annealing steps 9 and beyond all lasted (much) longer than 30 min. **b** Measured values of R as a function of the annealing steps listed in Table 1. The *dotted line* is the linear regressions obtained from the data of R in steps 8 to 16. The sheet resistance in Ω/square on the left-hand scale equals R multiplied by $\pi/\ln 2$

applied to arrive at the values reported in the abstract. A corresponding correction for the finite thickness of the film versus the point separation of 1 mm of the four-point probe is negligible [4, 5].

The general trends revealed by the two plots are as follows:

- Thermal annealing raises the room-temperature resistivity of the film irreversibly.
- A second or third annealing cycle at the same temperature and duration has a progressively smaller or no effect on the room-temperature resistivity (steps 2 vs. 3; steps 4 vs. 5 vs. 6; steps 7 vs. 8).
- Annealing at a temperature below the highest preceding one affects the resistivity insignificantly (steps 9 to 15 vs. 8), even for durations up to 12 times as long (steps 10 vs. 8).

Amorphous reactively sputtered films of tantalum, silicon, and nitrogen are part of a large class of amorphous ternary materials that all display high crystallization temperatures and structural stability [6]. One may therefore surmise that the irreversible rise of the resistivity reported here for the case of TaSiN applies to the whole class of reactively sputtered amorphous ternary films (such as TiSiN, WSiN, and WBN etc).

When exposed to heat from room temperature to 490 °C, the electrical resistivity of pure tantalum increases by 165 %. Upon cooling back to room temperature, the tantalum's electrical resistivity reverts to its initial room-temperature value. That of the amorphous $Ta_{42}Si_{13}N_{50}$ film investigated here does not, as the present results show. This irreversibility clearly must stem from an effect that differs from that of the ordinary temperature dependence of the electrical resistivity of metals.

4 Possible causes for the observation

Three obvious possibilities come to mind as causes for an irreversible change of the TaSiN film resistivity: changes (1) in film structure, (2) by chemical reaction of the film with the ambient, and (3) of the film stress.

4.1 Amorphous structure

The film is amorphous and is metastable with respect to crystallization. In electrically conducting amorphous structures, crystallization would typically decrease the electrical resistivity. However, the high metastability of TaSiN films mentioned initially [1–3] was established for annealing in vacuum, not in air. We present results that show that even after annealing in air, changes in the amorphous structure are undetectably small in the duration—temperature range considered here.

Figure 2 presents transmission-electron micrographs that were taken on films of the same batch of samples discussed in Sects. 2 and 3. The annealing in air of the analyzed film was performed twice at 500 °C for 30 min. The micrographs show that after this annealing, the structural changes are undetectably small (Figs. 2a vs 2b), even at high resolution (see Figs. 2c vs 2d). The electron diffraction rings (Figs. 2e vs 2f) confirm that the films are structurally amorphous

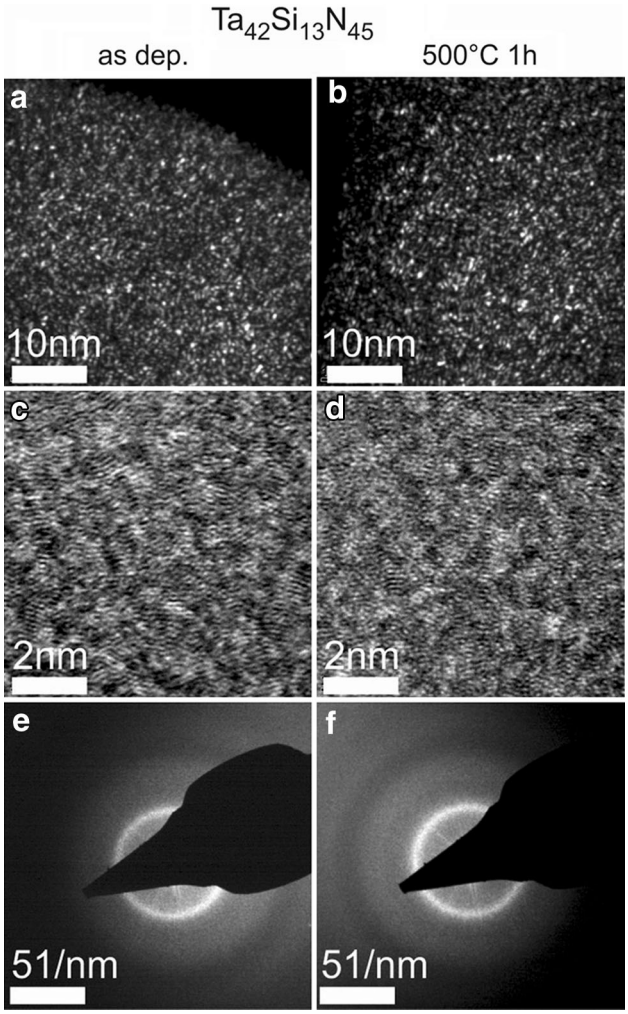

Fig. 2 Cross-sectional transmission electron micrographs and diffraction images. *Left* as-deposited $Ta_{42}Si_{13}N_{45}$ film. *Right* $Ta_{42}Si_{13}N_{45}$ film after thermal annealing in air at 500 °C for 60 min. *Top figures* cross-sectional transmission electron micrographs. *Central figures* high-resolution cross-sectional transmission electron micrographs. *Bottom figures* diffraction images of the films

initially and that they remain amorphous during the heat treatment. Furthermore, these micrographs are indistinguishable from those displayed in Ref. [3] for samples of a similar composition ($Ta_{36}Si_{14}N_{50}$) deposited in different sputtering systems and on different substrates. These results confirm once more that within a given composition range, the microstructure of reactively sputtered amorphous TaSiN films depends much less on the deposition conditions and on the composition ratios than is typically the case for the microstructure of polycrystalline films of alloys.

4.2 Chemical composition

The resistivity of the studied $Ta_{42}Si_{13}N_{45}$ films could also change upon thermal annealing by some chemical

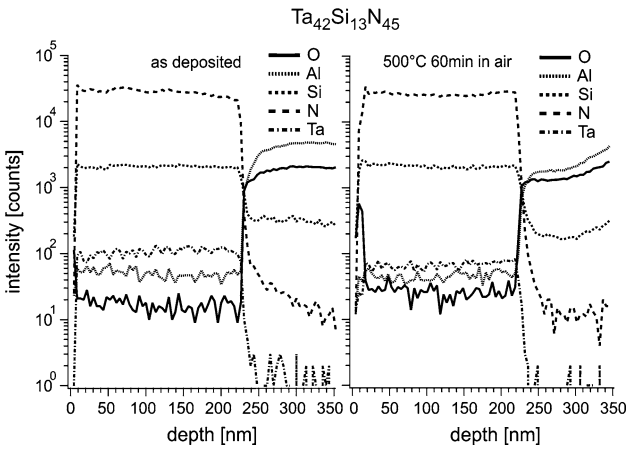

Fig. 3 Secondary-ion mass profiles. *Left* as-deposited $Ta_{42}Si_{13}N_{45}$ film. *Right* $Ta_{42}Si_{13}N_{45}$ film after thermal annealing in air at 500 °C for 60 min. Sputtering beam: Cs; analyzing beam: Ga. There is no perceptible penetration of oxygen into the films upon annealing. Only the surface oxidizes

interaction with air. Analyses by secondary-ion mass spectrometry of a pair of samples similar to those analyzed above show that the surface oxide thickens by less than 10 nm upon annealing in air at 500 °C twice for 30 min and that oxygen penetrates only imperceptibly into the bulk of the film (Fig. 3). In the process, the resistivity of the film rises by an amount consistent with the rise expected from Fig. 1. The results of the present secondary ion mass spectrometry analyses are consistent with previous investigations of the subject [7–10]. These studies all agree that at 500 °C TaSiN films in the composition range investigated here will minimally react with oxygen in air.

4.3 Stress state

If neither the structure nor the composition of the film change detectably upon thermal annealing in air, the third likely possible cause for an irreversible change of the film resistivity could be an irreversible change of the film stress. The following experiments demonstrate that the film stress does indeed change upon thermal annealing.

Reid has investigated experimentally how the compressive stress in reactively sputtered $Ta_{36}Si_{14}N_{50}$ films evolves during thermal annealing in air as a function of temperature [3]. Films about 400 nm thick were reactively deposited on polished 5 cm diameter (111) Si wafers 350 μm thick at an estimated temperature of about 100 °C. The stress in the film was then derived by tracking the radius of curvature of the sample as it was slowly heated in air at a rate of 3 °C/min from room temperature to 500 °C, kept there for 30 min, and was then allowed to cool again to room temperature.

The evolution of the stress of the film is depicted in Fig. 4. As deposited, the film on the silicon substrate

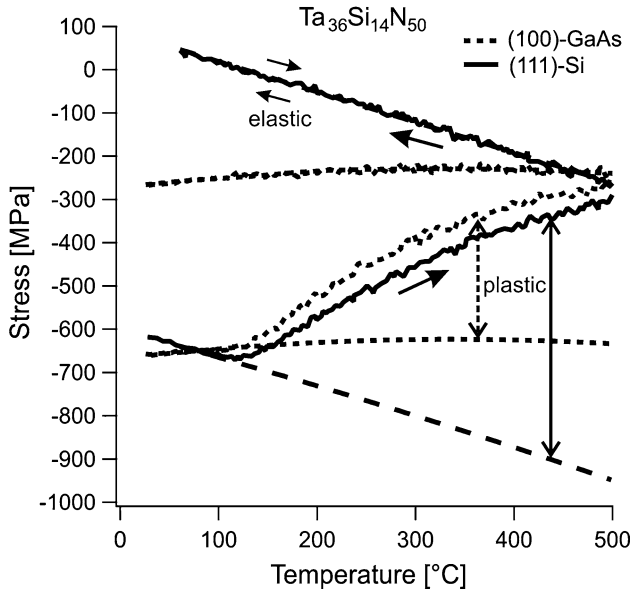

Fig. 4 Stress evolution of $Ta_{36}Si_{14}N_{50}$ films on (111) Si and (100) GaAs substrates. The *solid lines* describe how the compressive stress of reactively sputtered amorphous $Ta_{36}Si_{14}N_{50}$ films deposited on (111) Si and (100) GaAs substrates at about 100 °C changes as (1) the temperature slowly rises at a rate of 3 °C/min from room temperature to 500 °C, (2) the temperature remains steady there for 30 min, and (3) the sample cools down to room temperature again. On subsequent heating and cooling cycles, the system retraces the cooling curve, proving that the system responds elastically from then on up to ≤500 °C. The *vertical lines* indicate the total stress relaxation taking place at any given temperature during the first annealing cycle. *Solid lines* silicon substrate and *dashed lines* GaAs substrate. The *solid lines* for the silicon substrate (and the corresponding lines for the GaAs substrate) are experimental results published in Ref. [3]

(heavy lines) is under high isotropic compressive stress of about 600 MPa, a condition that is common in films deposited by sputtering. That stress is generally attributed to the peening process during sputter deposition [11]. One can distinguish four segments of stress changes in Fig. 4. When the temperature starts to rise, the compressive stress climbs first above its initial value of 600 MPa. This first segment can be explained by assuming that the $Ta_{36}Si_{14}N_{50}$ film expands thermally more than the silicon substrate does while their interface is mechanically locked. There follows a second segment of steady relaxation of the compressive stress of the film. At the temperature, maximum of 500 °C, the compressive film stress is roughly halved. During this third segment, the temperature remains steady at 500 °C for 30 min and the stress diminishes slightly by about 30 MPa (∼10 %). During the fourth segment of cooling, the film stress decreases monotonically and actually turns to a slightly tensile value at room temperature. This decline can again be explained by a dominant contraction of the film over that of the substrate. A quite revealing additional observation is that in a subsequent similar heating and cooling cycle, the stress–temperature response retraces that of the fourth segment of the initial cycle, as indicated by the two oppositely pointing arrows. The film-substrate system evidently responds elastically now and from then on. Another informative observation is that the slope of the initial rise of the compressive stress in the first segment of the initial annealing cycle matches closely that of the final segment. An extension of that initial rise of stress (dashed heavy line in Fig. 4) actually almost parallels the trace of the forth segment. This similarity leads to the idea that the interface between film and substrate actually remains mechanically locked during the whole annealing cycle. It then follows that the total compressive stress relaxed up to any temperature in the second segment of the initial cycle is that indicated by the length of the vertical solid line in Fig. 4. On the basis of these findings, it can also be understood that during any subsequent thermal cycling of the system that would not exceed the 500 °C of the first annealing cycle, the system will respond elastically and no further stress will relax. The initial climb of the compressive stress in the first segment of the first annealing cycle up to about 120 °C also makes sense. The film was deposited at about that temperature. As it subsequently cooled to room temperature, its stress decreased as it does when the system responds elastically.

Dauksher et al. [12] have also investigated the stress at room temperature in reactively sputtered amorphous $Ta_{61}Si_{17}N_{21}$ films 500 nm thick deposited on silicon wafers [12]. Their films had an initial compressive stress of 400 MPa and must have had a stress–temperature response closely resembling that for the $Ta_{42}Si_{13}N_{45}$ film on the silicon substrate in Fig. 4. They report that zero residual stress at room temperature is achieved after an annealing temperature of about 450 °C. That outcome is nicely compatible with the result of Fig. 4 considering that the deposition temperature of the films is not reported.

Reid repeated his experiment with the same amorphous reactively sputtered $Ta_{42}Si_{13}N_{45}$ film deposited on a (100) gallium arsenide wafer 475 μm thick and 5 cm in diameter [3]. The stress–temperature curves for the corresponding experiment performed on that system are reported in Fig. 4 as well (light dotted and dashed lines). The curves are qualitatively similar to those obtained with a silicon substrate, but with one noticeable difference. Below the deposition temperature of about 100 °C, the slopes of both the first and the fourth segments of the initial stress–temperature trace are positive and smaller in value than with silicon as a substrate. The difference can readily be attributed to the thermal expansion coefficient of gallium arsenide (6.8×10^{-6}/°C at 27 °C) that presumably exceeds that of the film but is closer to it than is that of silicon (2.6×10^{-6}/°C). Corresponding experiments with films of $W_{36}Si_{14}N_{50}$ on both silicon and gallium arsenide wafers yield results quite like those of the $Ta_{36}Si_{14}N_{50}$ film [3].

The linear thermal expansion coefficient of alumina is yet larger than that of gallium arsenide (between 6 and 8 ppm/°C depending on its density). The shape of the corresponding stress–temperature plot of the $Ta_{42}Si_{13}N_{45}$ film on an alumina substrate that is investigated in Sect. 3 will therefore resemble that of gallium arsenide in Fig. 4, assuming that the interface between film and substrate is again mechanically locked.

The elastic yield segments of the stress–temperature plot will then be steeper than those observed with the gallium arsenide substrate. Under such circumstances, it becomes unlikely that upon thermal annealing, an initially compressive stress would ever reverse to a tensile stress at room temperature.

5 Discussion

The way the resistivity of the amorphous $Ta_{36}Si_{14}N_{50}$ film changes at room temperature upon thermal annealing on an alumina substrate (Fig. 1) and the way the stress of the film changes at room temperature upon thermal annealing on a silicon and gallium arsenic substrate (Fig. 4) are strikingly similar. Both the resistivity and the stress change irreversibly upon thermal annealing above the deposition temperature. The new values remain unaltered as long as the temperature of any subsequent heat treatments does not exceed that of the previous annealing. If it does, both stress and resistivity at room temperature change irreversibly again. This same yet unusual pattern of behavior strongly suggests that stress and resistivity are two directly coupled phenomena in this reactively sputter-deposited amorphous TaSiN film. Stress is indeed commonly known to influence the resistivity of materials. In addition, the experimental data reported in sect. 4 identify film stress as the parameter most likely to affect the film resistivity during thermal annealing. However, the data presented here do not definitively establish that it is the relaxation of the film stress on the alumina substrate that alters the resistivity of the film because the stress evolution of the film has not been measured. Conversely, the change of stress of the film on silicon and gallium nitride has been tracked without simultaneously recording the change of the film resistivity. Yet we believe that this parallel and unusual behavior of stress and resistivity is unlikely to be simply coincidental. Instead, we claim that the reported evidence is convincing enough to posit that it is indeed the change of the film stress that alters the film resistivity. To establish a direct proof of that claim, the experiment that should follow this initial study should be to re-measure the changes of resistivity and of stress of the film on one and the same substrate at room temperature after thermal annealing. Until this proof exists, the present claim stands as a conjecture.

After the compressive stress is relaxed up to a given temperature (500 °C in the case of Fig. 4), the stress–temperature behavior becomes reversible up to that temperature. Within that temperature range, it is presumably the difference between the thermal expansion coefficients of the film and of the substrate that determines how the film stress—and hence the film resistivity—changes with temperature. When the substrate and the film expand thermally equally, the film resistivity would become temperature independent.

The model used here presumes that the interface between the film and the substrate is mechanically unyielding throughout the annealing process, i.e., the compressive stress relaxes within the bulk of the film, not at the interface between film and substrate. By our conjecture, the model applies equally to highly polished substrates of alumina, silicon, and gallium arsenide. Sputter deposition of films is an energetic process. Are the mechanically rigid interfaces inferred here a consequence of the particular procedure used to deposit the film? This is another provocative question raised by the present study. If it is so, the reactive sputter deposition procedure employed to synthesize the amorphous TaSiN film also affects the outcome of the present experiment. Insight could come from experiments executed with amorphous films deposited differently. Films of TiSiN [13, 14], of WBN [14, 15], and of WSiN [14], for example, have been formed by chemical vapor deposition. No measurements of the stress and of the resistivity as a function of temperature have been made on these films. Future experiments are required to clarify this issue.

Another realization is that to evaluate the properties of materials like reactively sputter-deposited amorphous TaSiN films, it is necessary to first sever the film from its substrate. The experiments described here do not provide such information.

It is instructive to evaluate how sensitive a reactively sputtered amorphous TaSiN film is to change in mechanical stress. Figure 5 plots the (irreversible) rise of the sheet resistivity at room temperature of a $Ta_{42}Si_{13}N_{45}$ film deposited on an alumina substrate against the stress induced by thermal annealing of a $Ta_{36}S_{14}N_{50}$ film deposited on a (100) GaAs wafer. Notice firstly that the two films differ slightly in composition. It is well established that the properties of amorphous reactively sputter-deposited films are insensitive to slight changes in composition. Secondly, the rise of the sheet resistivity was measured on a film deposited on an alumina substrate while the changes in film stress upon annealing were recorded for films deposited on silicon and on gallium arsenide wafers (Fig. 4). As mentioned in sect. 4, the stress–temperature plot for a reactively sputtered TaSiN film on an alumina substrate will resemble that of the same film on a gallium arsenide wafer. For that reason the abscissa of Fig. 5 is a

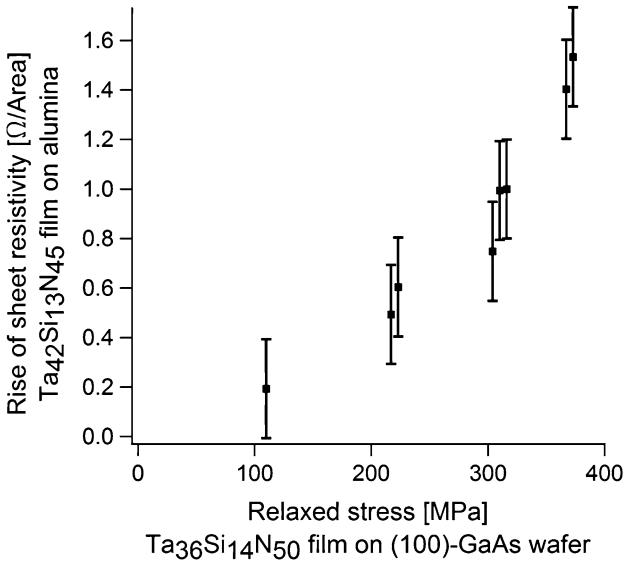

Fig. 5 Rise of the sheet resistivity (Ω/area) at room temperature of a $Ta_{42}Si_{13}N_{45}$ film deposited on an alumina substrate as a function of the relaxed amount of stress induced by thermal annealing of a $Ta_{36}Si_{14}N_{50}$ film deposited on a (100) GaAs wafer. The relaxed amount of stress is that labeled "plastic" at any given temperature in Fig. 4 for the case of the GaAs substrate. This value is that which would have been measured had the sample temperature been lowered to room temperature at that point in annealing process. The *error bars* indicate an estimated uncertainty of the reported values of the sheet resistivity in Fig. 1b

fair substitute for the case of an alumina substrate. Figure 5 thus approximates how stress and sheet resistivity relate to each other at room temperature for the case of a reactively sputtered amorphous TaSiN film on an alumina substrate. By our conjecture, this figure thus shows how changes in film stress affect the film's sheet resistivity at room temperature.

As can be seen, a positive stress raises the sheet resistivity of the film. This is so because a positive stress actually reduces the high initial compressive stress of the film. The stress affects the sheet resistivity monotonically, but non-linearly +100 MPa raise the sheet resistivity by +0.2 Ω/area, but the effect is about 5 times larger at +400 MPa. A model how the stress and the electrical resistivity evolve in amorphous reactively sputter-deposited TaSiN films is required to interpret this observation. That is another interesting topic raised by the present investigation. But data from of stress and resistivity performed on the same film/substrate combination must first exist.

6 Relevance of the results

The demonstrated high structural and chemical invariance of the TaSiN films makes them attractive as electronic elements exposed to harsh surroundings and/or to frequent temperature cycling. The results obtained here demonstrate, however, that the resistance of the film will stay reproducible only after the film has been pre-annealed above any anticipated future temperature exposure. This annealing process eliminates the deleterious role of the compressive stress accumulated in the film during its sputter deposition. For the present amorphous $Ta_{36}Si_{13}N_{45}$ film, the demonstrated useful range after pre-annealing is at least 500 °C and hours of operation in air.

7 Conclusion

It is conjectured that a change in the stress of reactively sputter-deposited amorphous TaSiN films (and presumably of any film of similar ternary composition) generates a change in the film's resistivity. Specifically, as the stress of the film declines irreversibly, the electrical resistivity of the film rises, also irreversibly. How these changes evolve depends on both the film and the substrate. The demonstrated high structural and chemical resistance of these films in air makes them attractive as electronic elements exposed to harsh surroundings and/or to frequent temperature cycling. However, a reproducible resistivity of the film as a function of temperature will only be assured after the film has been pre-annealed above any anticipated future temperature exposure.

We cannot compare our results with data from the open literature. To our knowledge, similar information on the resistivity and the stress of amorphous reactively sputter-deposited films as are presented here do not exist.

Acknowledgments The $Ta_{36}Si_{14}N_{50}$ film was deposited and patterned by Dietmar Bertsch at NTB, Buchs (SG). Peter van der Wal and Sylviane Pochon of the IMT, University of Neuchâtel, sliced the alumina substrate. The secondary ion mass profiles reproduced in Fig. 3 were obtained from Jen-Sue Chen, Natl. Cheng Kung University, Taiwan. Konrad Samwer, University of Göttingen, offered constructive suggestions how to better the manuscript (e.g. Fig. 5). We thank them all five for their generous participation.

References

1. E. Kolawa, J.M. Molarius, C.W. Nieh, M.-A. Nicolet, J. Vac. Sci. Technol. A **8**(3), 3006 (1990)
2. J.S. Reid, E. Kolawa, R.P. Ruiz, M.-A. Nicolet, Thin Solid Films **236**, 319 (1993)
3. J.S. Reid, Ph.D. thesis California Institute of Technology, USA, 1995
4. F.M. Smits, Bell Syst. Tech. J. **37**(3), 711 (1958)
5. M.A. Green, M.W. Gunn, Solid State Electron. **14**, 1167 (1971)
6. M.-A. Nicolet, P.H. Giauque, Microelectron. Eng. **55**, 357 (2001)
7. P.J. Pokela, J.S. Reid, C.K. Kwok, E. Kolawa, M.-A. Nicolet, J. Appl. Phys. **70**(5), 2828 (1991)
8. T. Hara, M. Tanaka, K. Sakiyama, S. Onishi, K. Ishihara, J. Kudo, Jpn. J. Appl. Phys. Part 2, Lett. **36**(7B), L839 (1997)

9. A. Grill, C. Jahnes, C. Cabral Jr, J. Mater. Res. **14**(4), 1604 (1999)
10. C. Cabral Jr, K.L. Saenger, D.E. Kotecki, J.M.E. Harper, J. Mater. Res. **15**(1), 194 (2000)
11. H. Windischmann, Crit. Rev. Solid State Mater. Sci. **17**(6), 547 (1992)
12. W.J. Dauksher, D.J. Resnick, K.D. Cummings, J. Baker, R.B. Gregory, N.D. Theodore, J.A. Chan, W.A. Johnson, C.J. Mogab, M.-A. Nicolet, J.S. Reid, J. Vac. Sci. Technol. **B13**(6), 3103 (1995)
13. P.M. Smith, J.S. Custer, R.V. Jones, A.W. Maverick, D.A. Roberts, J.A.T. Norman, A.K. Hochberg, G. Bai, J.S. Reid, M.-A. Nicolet, in *Conference Proceedings ULSI XI Materials Research Society*, vol 249 (1996)
14. J.G. Fleming, P.M. Smith, J.S. Custer, E. Roherty-Osmun, M. Cohn, R.V. Jones, D.A. Roberts, J.A.T. Norman, A.K. Hochberg, J.S. Reid, Y.-D. Kim, T. Kacsich, M.-A. Nicolet, in *Conference Proceedings ULSI XII Materials Research Society*, vol 249 (1997)
15. J.G. Fleming, E. Roberty-Osmun, P.M. Smith, J.S. Custer, Y.-D. Kim, T. Kacsich, M.-A. Nicolet, C.J. Galewski, Thin Solid Films **320**, 10 (1998)